Extracellular vesicle therapeutics for cardiac repair: A translational perspective

Mol, E.A.

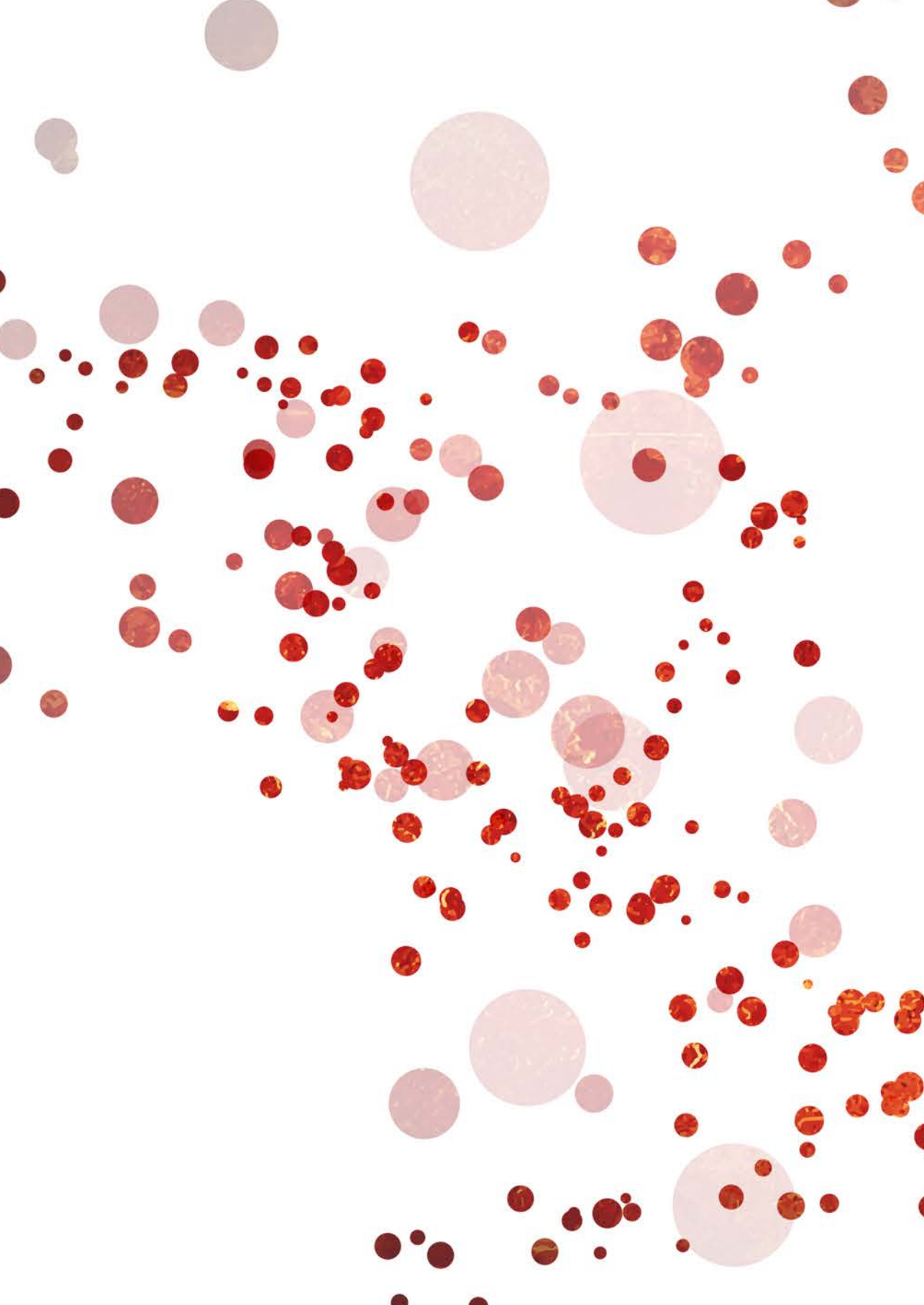

CHAPTER 2

Higher functionality of extracellular vesicles isolated using size-exclusion chromatography compared to ultracentrifugation

Emma A. Mol MSc[1,2], Marie-José Goumans PhD[2], Pieter A. Doevendans PhD[1,3,4], Joost P.G. Sluijter PhD[1,3,4], Pieter Vader PhD[5]

Nanomedicine 2017; 13: 2061-2065

[1] Department of Cardiology, Laboratory of Experimental Cardiology, University Medical Center Utrecht, Utrecht 3584CX, The Netherlands
[2] Laboratory of Cardiovascular Cell Biology, Department of Cell and Chemical Biology, Leiden University Medical Center, Leiden 2333ZA, The Netherlands
[3] UMC Utrecht Regenerative Medicine Center, University Medical Center, Utrecht 3584CT, The Netherlands
[4] Netherlands Heart Institute (ICIN), Utrecht 3584CX, The Netherlands
[5] Laboratory of Clinical Chemistry and Haematology, University Medical Center Utrecht, Utrecht 3584, The Netherlands

ABSTRACT

Extracellular vesicles (EVs) are nano-sized, lipid bilayer-enclosed particles involved in intercellular communication. EVs are increasingly being considered as drug delivery vehicles or as cell-free approach to regenerative medicine. However, one of the major challenges for their clinical application is finding a scalable EV isolation method that yields functional EVs. Although the golden standard for EV isolation is ultracentrifugation (UC), a recent study suggested that isolation using size-exclusion chromatography (SEC) yielded EVs with more intact biophysical properties. Whether this also leads to differences in functionality remained to be investigated. Therefore, we investigated possible differences in functionality of cardiomyocyte progenitor cell-derived EVs isolated using UC and SEC. Western blot analysis showed higher pERK/ERK ratios after stimulation with SEC-EVs compared to UC-EVs, indicating that SEC-EVs bear higher functionality. Therefore, we propose to use SEC-EVs for further investigation of EVs' therapeutic potential. Further optimization of isolation protocols may accelerate clinical adoption of therapeutic EVs.

BACKGROUND

Extracellular vesicles (EVs) are nano-sized endogenous messengers containing a plethora of biological cargo including proteins and RNA, reflecting the content of the secreting cell. By mediating intercellular communication, EVs can influence recipient cell behavior, and affect physiological and pathological processes[1–3]. For this reason, EVs are increasingly being considered for therapeutic purposes, including cell-free approaches for regenerative medicine and drug delivery[4–6]. The interest in using EVs for cardiac therapy increased after it became clear that the beneficial effects of stem cell therapy after a myocardial infarction (MI) were mainly due to paracrine actions[7]. EVs were identified to be the major component of the stem cell secretome responsible for the observed increase in cardiac function[8]. Therefore, using EVs as an off-the-shelf therapeutic may circumvent some of the drawbacks of cell based therapy, such as cell survival, retention, rejection, and the use of replicating cells.

One of the major challenges for implementation of EVs as therapeutics is the development of a scalable, reproducible, and standardisable isolation method that results in an acceptable yield of EVs. To date, the most common EV isolation method is differential ultracentrifugation (UC). This method relies on sedimentation at high speed for separating EVs from other (extra)cellular components. Although the UC protocol is relatively straightforward, it is also time consuming, and may yield aggregated EVs after pelleting[9,10]. Furthermore, UC isolation results in low and operator-dependent yields and EVs can be damaged due to shearing forces, as a result of centrifugation at high speeds[11,12]. An additional method for EV isolation, based on ultrafiltration and size-exclusion chromatography (SEC) to separate EVs from other media components, was recently suggested by Nordin et al[13]. EVs isolated using chromatography (SEC-EVs) are more intact than EVs isolated using UC (UC-EVs), likely due to the absence of centrifugation at high speeds. Whether this also leads to differences in functionality of SEC- and UC-EVs remained to be investigated.

RESULTS

In order to investigate whether the isolation protocol affects EV functionality, EVs derived from cardiomyocyte progenitor cells (CPCs) were isolated using UC and SEC. CPCs are being intensively investigated for cardiac-related therapies, and CPC-derived EVs have previously been shown to bear pro-angiogenic properties[14–16]. A schematic representation of the UC and SEC isolation protocols used in this study is shown in Figure 1.

First, EV yield was compared by quantification of EV protein content and number of particles, as shown in Figure 2A. No significant differences in total EV protein or particle yield between UC and SEC were found. This is in contrast with previous observations showing that SEC isolation results in a higher EV yield compared to UC isolation.[13] This may be explained by variation between cell types or due to slight differences in UC or SEC isolation procedure (e.g. rotor/filter type or pore size). Next, UC-EVs and SEC-EVs were characterized based on size distribution, morphology, and the presence or absence of protein markers. Figure 2B shows a representative size distribution profile of UC-EVs and SEC-EVs based on Nanoparticle Tracking Analysis. SEC-EVs had a smaller size distribution with the highest peak at

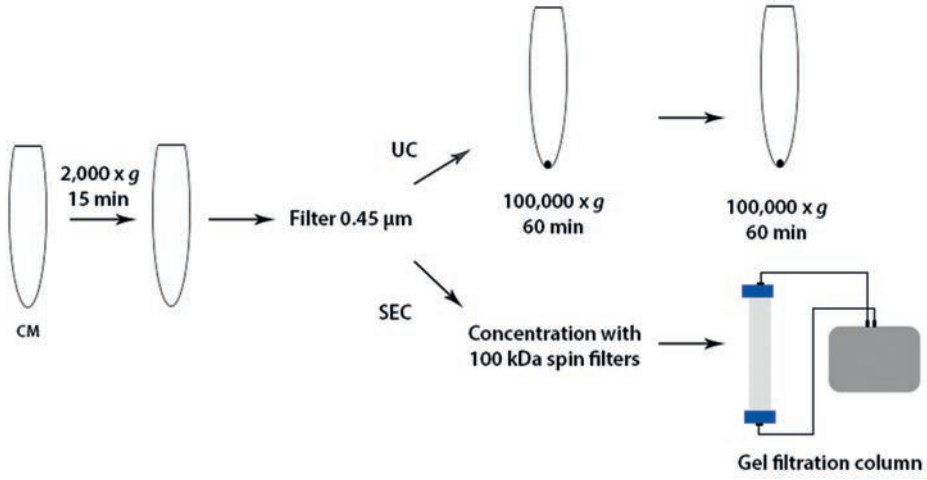

Figure 1 Schematic overview of EV isolation protocols used in this study.
Abbreviations: CM = conditioned medium, SEC = size-exclusion chromatography, UC = ultracentrifugation.

approximately 90 nm, compared to a broader size range for UC-EVs, peaking at approximately 100 nm. Transmission electron microscopy analysis showed no major morphological differences between UC-EVs and SEC-EVs, as both preparations contained both smaller and larger vesicles (Figure 2C). Western Blot analysis revealed that both UC-EVs and SEC-EVs were enriched for EV marker proteins Alix and CD63, but not TSG101 (Figure 2C). Although the expected band for Alix (96 kDa) was present for both UC-EVs and SEC-EVs, an extra band at 90 kDa was observed in the UC-EV preparation. The presence of double bands for Alix may be explained by differential phosphorylation status, as Alix is known to have multiple phosphorylation sites[17]. Why this second band was exclusively found in UC-EVs remains unclear, but might suggest a different vesicle sub-class or activation status. The endoplasmatic reticulum protein calnexin was only detected in the cell lysate, confirming the absence of contamination with other membrane compartments in EVs. β-actin was found in similar levels in EVs and cell lysate.

CPC-derived EVs have previously been shown to stimulate migration of human microvascular endothelial cells (HMECs) in a scratch wound assay[14]. As the mitogen-activated protein kinase1/2 (MAPK1/2) – extracellular signal-regulated kinase1/2 (ERK1/2) pathway is known to play an important role in cell survival, migration and angiogenesis during wound healing[18–20], EV-induced ERK1/2 phosphorylation was used as a read-out to evaluate the possible differences in functionality of UC-EVs and SEC-EVs. To investigate the functionality of EV preparations, HMECs were stimulated with UC-EVs and SEC-EVs (Figure 3A).

Due to a lack of consensus in the EV-field on the most accurate method for EV quantification, HMECs were stimulated with both equal amounts of UC-EV and SEC-EV protein (Figure 3B), and equal numbers of EV particles (Figure 3C). Levels of phosphorylated ERK1/2 and total ERK1/2 were determined using western blotting, after which pERK/ERK ratios were calculated. A dose-dependent increase in ERK phosphorylation was observed for SEC-EVs, as treatment

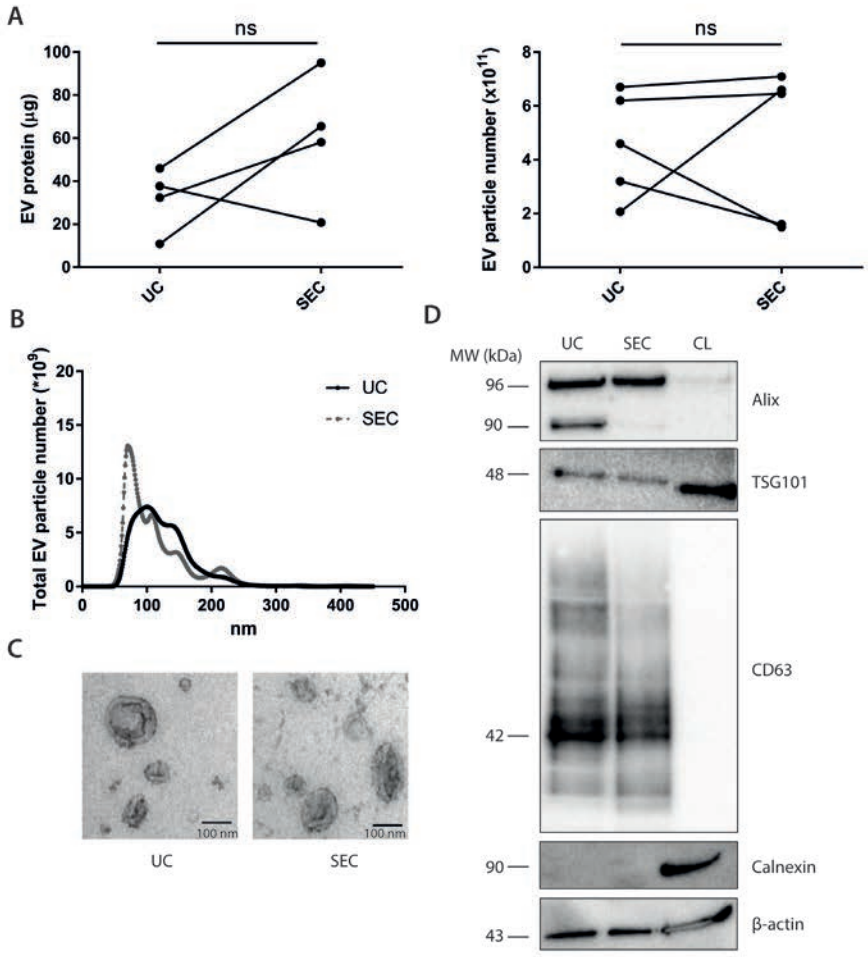

Figure 2 Characterization of UC-EVs and SEC-EVs.
A) EV yield as determined by microBCA analysis (EV protein, upper panel) and Nanoparticle Tracking Analysis (NTA) (EV particle number, lower panel). Statistical analysis was performed using an unpaired student's t-test. B) Size distribution profile of UC-EVs and SEC-EVs as determined by NTA. C) Transmission electron microscopy pictures of UC-EVs and SEC-EVs. Scale bar = 100 nm. D) Western Blot of UC-EVs, SEC-EVs and cell lysate (CL). Abbreviations: CL = cell lysate, MW = molecular weight, SEC = size-exclusion chromatography, UC = ultracentrifugation.

with 3 µg SEC-EVs led to a higher pERK/ERK ratio compared to 1 µg SEC-EVs (2.1±0.3 for 3 µg SEC-EVs vs 1.2±0.2 for 1 µg SEC-EVs). Moreover, stimulation with 3 µg SEC-EVs resulted in a higher pERK/ERK ratio compared to stimulation with 3 µg of UC-EVs (2.1±0.3 for SEC-EVs vs 1.0±0.2 for UC-EVs). The same trend was observed after adding equal numbers of EV particles to HMECs (Figure 3C). Stimulation of HMECs with 6.10^{10} SEC-EVs resulted in higher pERK/ERK ratio compared to 6.10^{10} UC-EVs (3.56±1.29 for SEC particles vs 1.42±0.24 for UC particles). These results show that CPC-derived SEC-EVs have higher functionality compared to UC-EVs.

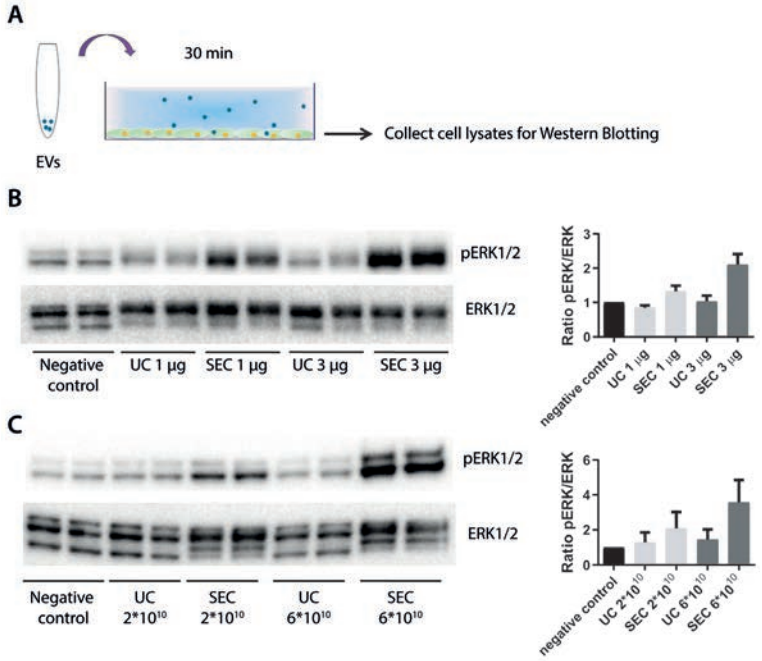

Figure 3 Assessment of UC-EV and SEC-EV functionality.
A) HMECs were stimulated with EVs for 30 minutes, after which phosphorylated ERK1/2 and total ERK1/2 protein levels were determined using Western Blotting. B) Stimulation of HMECs with equal amounts of UC-EV and SEC-EV protein. C) Stimulation with equal numbers of UC-EV and SEC-EV particles. Abbreviations: ERK = extracellular signal-regulated kinase, SEC = size-exclusion chromatography, UC = ultracentrifugation.

DISCUSSION

The striking difference in functionality between UC-EVs and SEC-EVs may result from the high shear forces that are applied during high speed centrifugation during UC isolation. These may detrimentally affect signaling molecules on the EV surface, thereby preventing UC-EVs to activate, bind to or be taken up by recipient cells. Indeed, UC-EVs have previously been described to appear ruptured when studied using transmission electron microscopy and fluorescence correlation spectroscopy[13]. Furthermore, the size distribution profile of SEC-EVs also differed from UC-EVs, as SEC-EVs were found to be smaller in size compared to UC-EVs. The apparent larger size may be the result of aggregation or fusion of EVs during UC, as also suggested by others[9,11,13]. Alternatively, UC isolation may enrich for larger EVs that sediment more efficiently. Whether and how this contributes to EV functionality remains to be investigated. Furthermore, as characteristics of isolated EVs vary between cell types, differences in functionality between SEC-EVs and UC-EVs may be cell type-dependent. This needs to be addressed in future studies.
In this study, we used induction of ERK phosphorylation as an outcome parameter to assess EV functionality, as activation of HMECs via pERK has been shown to be indicative for the

angiogenic potential of EVs[15]. One could argue that SEC-EVs may be contaminated with other soluble materials that affect ERK phosphorylation. Although we cannot exclude this completely, Western Blot analyses as well as protein and particle number measurements indicate that SEC isolation allows for EV preparations with similar purity as UC (Figure 1A,D). Additionally, CPC-EVs may affect other processes involved in cardiac disease, as treatment with CPC-EVs has been shown to result in increased cardiac function after MI in mice by enhancing angiogenesis, as well as reducing cardiomyocyte apoptosis[16]. Whether SEC-EVs display increased functionality for cardiac repair *in vivo*, as well as for other therapeutic strategies, therefore remains to be investigated.

In conclusion, one of the major challenges for developing EV therapeutics is finding a scalable isolation method that yields EVs with high functionality. Although previous reports already suggested that EV function might be affected by the isolation procedure, to our knowledge, we are the first to show that EV isolation technique can actually affect their functionality. SEC isolation results in more functional EVs compared to UC isolation, which is especially important when developing EVs as therapeutics.

Acknowledgements

The authors thank Sander van de Weg (UMC Utrecht) for excellent assistance with electron microscopy. EAM is supported by the Project SMARTCARE-II of the BioMedicalMaterials institute, co-funded by the ZonMw-TAS program (#116002016), the Dutch Ministry of Economic Affairs, Agriculture and Innovation and the Netherlands CardioVascular Research Initiative (CVON): the Dutch Heart Foundation, Dutch Federations of University Medical Centers, the Netherlands Organization for Health Research and Development, and the Royal Netherlands Academy of Sciences. PV is funded by a VENI fellowship (#13667) from the Netherlands Organisation for Scientific Research (NWO). The authors declare no conflicts of interest.

REFERENCES

1. Valadi, H. *et al.* Exosome-mediated transfer of mRNAs and microRNAs is a novel mechanism of genetic exchange between cells. *Nat. Cell Biol.* **9**, 654–9 (2007).
2. Ratajczak, J. *et al.* Embryonic stem cell-derived microvesicles reprogram hematopoietic progenitors: evidence for horizontal transfer of mRNA and protein delivery. *Leukemia* **20**, 847–56 (2006).
3. Skog, J. *et al.* Glioblastoma microvesicles transport RNA and proteins that promote tumour growth and provide diagnostic biomarkers. *Nat. Cell Biol.* **10**, 1470–6 (2008).
4. Sluijter, J. P. G., Verhage, V., Deddens, J. C., van den Akker, F. & Doevendans, P. A. Microvesicles and exosomes for intracardiac communication. *Cardiovasc. Res.* **102**, 302–11 (2014).
5. Haney, M. J. *et al.* Exosomes as drug delivery vehicles for Parkinson's disease therapy. *J. Control. Release* **207**, 18–30 (2015).
6. Julich, H., Willms, A., Lukacs-Kornek, V. & Kornek, M. Extracellular vesicle profiling and their use as potential disease specific biomarker. *Front. Immunol.* **5**, 413 (2014).
7. Timmers, L. *et al.* Human mesenchymal stem cell-conditioned medium improves cardiac function following myocardial infarction. *Stem Cell Res.* **6**, 206–14 (2011).
8. Lai, R. C. *et al.* Exosome secreted by MSC reduces myocardial ischemia/reperfusion injury. *Stem Cell Res.* **4**, 214–22 (2010).
9. Linares, R., Tan, S., Gounou, C., Arraud, N. & Brisson, A. R. High-speed centrifugation induces aggregation of extracellular vesicles. *J. Extracell. vesicles* **4**, 29509 (2015).
10. Bobrie, A., Colombo, M., Krumeich, S., Raposo, G. & Théry, C. Diverse subpopulations of vesicles secreted by different intracellular mechanisms are present in exosome preparations obtained by differential ultracentrifugation. *J. Extracell. vesicles* **1**, (2012).
11. Lamparski, H. G. *et al.* Production and characterization of clinical grade exosomes derived from dendritic cells. *J. Immunol. Methods* **270**, 211–226 (2002).
12. Taylor, D. D. & Shah, S. Methods of isolating extracellular vesicles impact down-stream analyses of their cargoes. *Methods* **87**, 3–10 (2015).
13. Nordin, J. Z. *et al.* Ultrafiltration with size-exclusion liquid chromatography for high yield isolation of extracellular vesicles preserving intact biophysical and functional properties. *Nanomedicine* **11**, 879–83 (2015).
14. Vrijsen, K. R. *et al.* Cardiomyocyte progenitor cell-derived exosomes stimulate migration of endothelial cells. *J. Cell. Mol. Med.* **14**, 1064–1070 (2010).
15. Vrijsen, K. R. *et al.* Exosomes from Cardiomyocyte Progenitor Cells and Mesenchymal Stem Cells Stimulate Angiogenesis Via EMMPRIN. *Adv. Healthc. Mater.* **5**, 2555–2565 (2016).
16. Barile, L. *et al.* Extracellular vesicles from human cardiac progenitor cells inhibit cardiomyocyte apoptosis and improve cardiac function after myocardial infarction. *Cardiovasc. Res.* **103**, 530–541 (2014).
17. Watson, D. C. *et al.* Efficient production and enhanced tumor delivery of engineered extracellular vesicles. *Biomaterials* **105**, 195–205 (2016).
18. Ballif, B. A. & Blenis, J. Molecular mechanisms mediating mammalian mitogen-activated protein kinase (MAPK) kinase (MEK)-MAPK cell survival signals. *Cell Growth Differ.* **12**, 397–408 (2001).
19. Eliceiri, B. P., Klemke, R., Strömblad, S. & Cheresh, D. A. Integrin alphavbeta3 requirement for sustained mitogen-activated protein kinase activity during angiogenesis. *J. Cell Biol.* **140**, 1255–63 (1998).
20. Alavi, A., Hood, J. D., Frausto, R., Stupack, D. G. & Cheresh, D. A. Role of Raf in vascular protection from distinct apoptotic stimuli. *Science* **301**, 94–6 (2003).
21. Smits, A. M. *et al.* Human cardiomyocyte progenitor cells differentiate into functional mature cardiomyocytes: an *in vitro* model for studying human cardiac physiology and pathophysiology. *Nat. Protoc.* **4**, 232–243 (2009).

SUPPLEMENTAL METHODS

Cell culture

CPCs and HMECs were cultured in the appropriate cell culture medium[14,21]. For EV isolation, CPCs were cultured for 3 days, after which medium was replaced with serum-free Medium 199 (Gibco, 31150-022). Conditioned medium (CM) from approximately 400 million cells was collected after 24 hours. Cells were passaged at 80-90% confluency using 0.25% trypsin digestion, and all cells were incubated at 37°C (5% CO_2 and 20% O_2).

EV isolation protocol

EVs were isolated using ultracentrifugation (UC) and ultrafiltration combined with size-exclusion chromatography (SEC). Cell culture CM was precleared from debris by centrifugation at 2000 x *g* for 15 min, followed by filtration (0.45 µm). Next, CM was divided for the two isolation techniques. For UC, CM was centrifuged using a type 50.2 Ti fixed-angle rotor for 1 hour at 100.000 x *g* to pellet EVs, and washed with phosphate buffer by centrifugation at 100.000 x *g* subsequently. For SEC, CM was concentrated using 100-kDA molecular weight cut-off (MWCO) Amicon spin filters (Merck Millipore). Subsequently, concentrated CM was loaded onto a S400 highprep column (GE Healthcare, Uppsala, Sweden) using an AKTAStart (GE Healthcare) containing a UV 280nm flow cell. The EV-containing fractions were pooled after elution and concentrated using a 100-kDa MWCO Amicon spin filter. Both EV preparations were filtered (0.45 µm) afterwards. The particle amount and size distribution were measured using Nanoparticle Tracking Analysis (Nanosight NS500, Malvern) with the camera level set at 15, and the detection threshold at 5. Protein content was determined using a microBCA protein assay kit™ (Thermo Scientific). Transmission electon microscopy pictures were made with a FEI Tecnai™ transmission electron microscope.

Assessment of EV functionality

First, HMECs were starved in basal MCDB-131 medium for 3 hours. Next, HMECs were either stimulated with equal amounts EV protein (1 or 3 µg) or equal amounts of EV particles ($2*10^{10}$ or $6*10^{10}$ particles) for 30 minutes, after which cells were lysed using lysis buffer (Roche, 04719964000). Cell lysates were centrifuged for 10 minutes at 14.000 x *g*, and phosphorylated ERK1/2 and total ERK1/2 protein levels were determined using Western Blotting.

Western blotting

Proteins were loaded on pre-casted Bis-Tris protein gels (ThermoFischer, NW04125BOX) for 1 hour at 160V, after which proteins were transferred to PVDF membranes (Millipore, IPVH00010). After incubation with antibodies for 42/44 pERK1/2 (Cell Signaling, 43705), 42/44 ERK1/2 (Cell Signaling, 91025), Alix (Abcam, 177840), TSG101 (Abcam, 30871), CD63 (Abcam, 8219), Calnexin (Tebu-bio, GTX101676), or β-actin (Sigma, A5441) a chemiluminescent peroxidase substrate (Sigma, CPS1120) was used to visualize the proteins. Quantification of the images was performed using ImageJ software (1.47V).

Statistical analysis

Data are presented as mean ± SEM. Student's t-test was used for comparison of two groups. A significance level of $p<0.05$ was used for the analysis.